Toward Perceiving Robots as Humans: Three Handshake Models Face the Turing-Like Handshake Test

Guy Avraham, Ilana Nisky, Hugo L. Fernandes, Daniel E. Acuna, Konrad P. Kording, Gerald E. Loeb, *Senior Member*, *IEEE*, and Amir Karniel, *Senior Member*, *IEEE*

Abstract—In the Turing test a computer model is deemed to "think intelligently" if it can generate answers that are indistinguishable from those of a human. We developed an analogous Turing-like handshake test to determine if a machine can produce similarly indistinguishable movements. The test is administered through a telerobotic system in which an interrogator holds a robotic stylus and interacts with another party—artificial or human with varying levels of noise. The interrogator is asked which party seems to be more human. Here, we compare the human-likeness levels of three different models for handshake: 1) Tit-for-Tat model, 2) λ model, and 3) Machine Learning model. The Tit-for-Tat and the Machine Learning models generated handshakes that were perceived as the most human-like among the three models that were tested. Combining the best aspects of each of the three models into a single robotic handshake algorithm might allow us to advance our understanding of the way the nervous system controls sensorimotor interactions and further improve the human-likeness of robotic handshakes.

Index Terms—Handshake, sensorimotor control, psychophysics, teleoperation, turing test.

1 Introduction

Machines are being used increasingly to replace humans in various tasks such as preparing food, communicating, and remembering. Personal assistive robots are a promising mean to deal with the large increase in the ratio of retirees to workers in most industrialized societies. Semi or fully automatically controlled robots may be used as coworkers with humans to perform dangerous and monotonous jobs, such as lifting heavy objects on a production line. From a medical point of view, personal assistive robots can be most useful with helping motorically impaired patients in performing various tasks such as encouraging a stroke patient to do rehabilitation, helping a Parkinson patient to pick up a cup of coffee, etc. When such robots interact physically with humans, they will need to be capable of human-like nonverbal communication such as the natural tendency of cooperating humans to synchronize their movements.

From a sensorimotor perspective, handshake is one of the simplest and most common sensorimotor interactions. It is characterized by the synchronization of the participants' hand motions, which must necessarily be in phase. From a cognitive standpoint, the handshake is considered to be a very complex process. Humans use their observations during handshake to make judgments about the personality of new acquaintances [1], [2]. Thus, by its bidirectional nature, in which both sides actively shake hands, this collaborative sensorimotor behavior allows the two participants to communicate and learn about each other.

Around 1950, Turing proposed his eponymous test for evaluating the intelligence of a machine, in which a human interrogator is asked to distinguish between answers provided by a person and answers provided by a computer. If the interrogator cannot reliably distinguish the machine from the human, then the machine is said to have passed the test [3]. Here, we present a Turing-like handshake test for sensorimotor intelligence. We expect this test to help in the design and construction of mechatronic hardware and control algorithms that will enable generating handshake movements indistinguishable from those of a human. We define the term "sensorimotor intelligence" as the sensorimotor version of the "artificial intelligence" that Turing aimed to explore in his test. In the original concept for this test, the interrogator generates handshake movements through a telerobotic interface and interacts either with another human, a machine, or a linear combination of the two (Fig. 1) [4], [5], [6], [7], [8]. We aimed to design the experiment such that the interrogator's judgments were based only on the

- *G. Avraham and A. Karniel are with the Department of Biomedical Engineering, Ben-Gurion University of the Negev, Beer-Sheva, Israel. E-mail: {guyavr, akarniel}@bgu.ac.il.*
- *I. Nisky is with the Department of the Mechanical Engineering, Stanford University, 424 Panama Mall, Building 560, Room 116, Stanford, CA 94305 and the Department of Biomedical Engineering, Ben-Gurion University of the Negev, Beer-Sheva, Israel. E-mail: nisky@stanford.edu.*
- *H.L. Fernandes and D.E. Acuna are with the Department of Physical Medicine and Rehabilitation, Rehabilitation Institute of Chicago, Northwestern University, 345 E. Superior Street, Kording Lab, Rm 1479, Chicago, IL 60611. E-mail: hugoguh@gmail.com, acuna002@umn.edu.*
- *K.P. Kording is with the Department of Physical Medicine and Rehabilitation, Rehabilitation Institute of Chicago, Northwestern University, 5617 S. Harper Avenue, Chicago, IL 60637. E-mail: koerding@gmail.com.*
- *G.E. Loeb is with the Department of Biomedical Engineering, University of Southern California, Denney Research Building, Room B-11, 1042 Downey Way, Los Angeles, CA 90089-1112. E-mail: gloeb@usc.edu.*

Manuscript received 29 Nov. 2011; revised 27 Mar. 2012; accepted 1 Apr. 2012; published online 10 Apr. 2012.
Recommended for acceptance by M. Flanders.
For information on obtaining reprints of this article, please send e-mail to: toh@computer.org, and reference IEEECS Log Number THSI-2011-11-0095.
Digital Object Identifier no. 10.1109/ToH.2012.16.

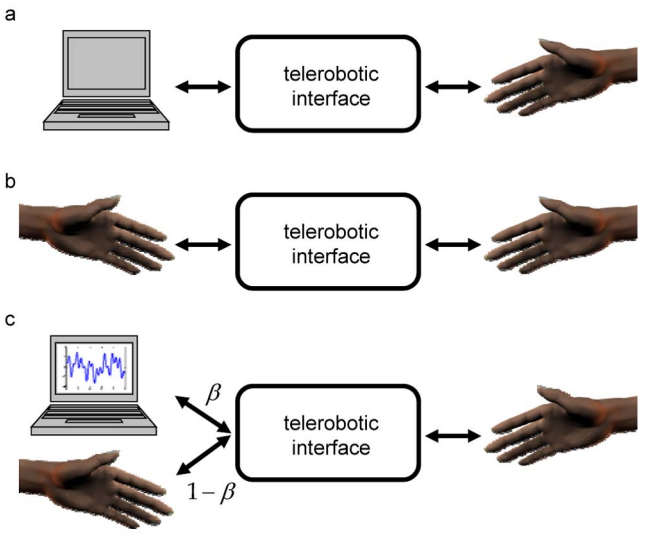

Fig. 1. Illustration of the handshake test. The human interrogator (right) was presented with simulated handshakes (a), natural handshakes (b), or a linear combination of human handshake and noise (c). After two interactions the interrogator had to choose which of the handshakes was more human-like.

sensorimotor interaction with the telerobotic interface (a Phantom Desktop haptic device from Sensable Technologies in the current study) and not on additional cues. In this context, the telerobotic interface is necessary for controlling the nature of the information available to the human interrogator, much as the teletype was necessary for hiding the physical computer from the questioning human in the original Turing test.

Obviously, an ultimate Turing-like test for sensorimotor intelligence involves an enormous repertoire of movements. We used a reduced version of the test that is based on a 1D handshake test proposed and developed in previous studies [4], [5], [6], [7], [8]. We used the same quantitative measure for human-likeness of a handshake model, the Model Human-Likeness Grade (MHLG). This grade quantifies the human-likeness on a scale between 0 and 1 based on the answers of the human interrogator, who compares the artificial handshake to the human handshake degraded with varying amounts of noise [5], [7].

Although there is a growing interest in improving human-likeness of mechatronic systems [9], [10], [11], [12], [13], [14], [15], [16], [17], [18], [19], [20], the development of artificial handshake systems is still in its infancy [21], [22], [23], [24], [25], [26], [27], [28]. Research on human sensorimotor control has generated many theories about the nature of hand movements [29], [30], [31], [32], [33], [34], [35], [36], [37], [38], [39], [40], [41], [42]. The proposed Turing-like handshake test can be useful for testing those theories. In general terms, we assert that a true understanding of the sensorimotor control system could be demonstrated by building a humanoid robot that is indistinguishable from a human in terms of its movements and interaction forces. A measure of how close such robots are to this goal should be useful in evaluating current scientific hypotheses and guiding future neuroscience research. Here, we present the results of a Turing-like handshake test minitournament, in which we compared three selected different models for handshake: 1) the tit-for-tat model, according to which we identified active-passive

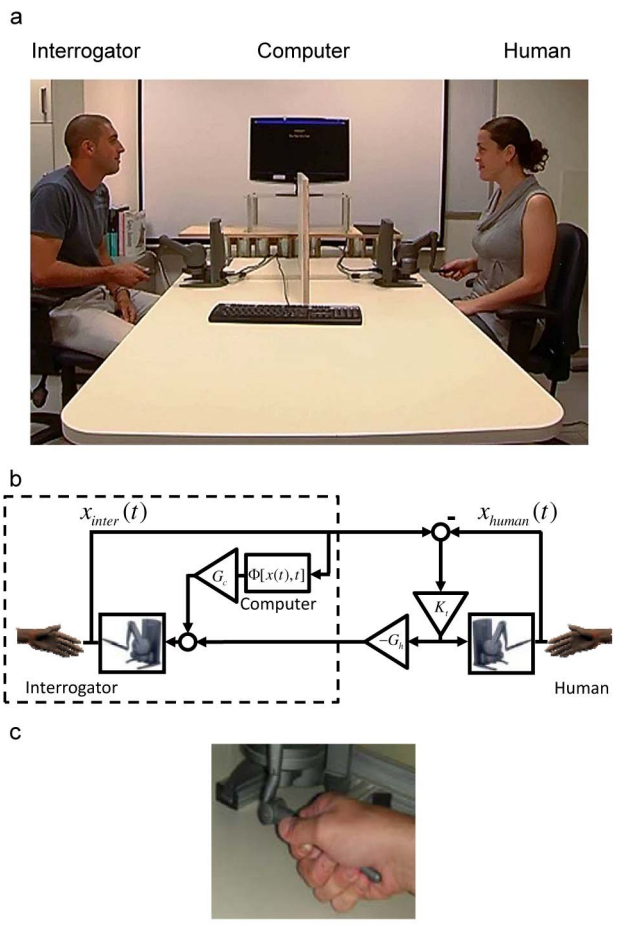

Fig. 2. The Turing-like handshake test for sensorimotor intelligence was administered through a telerobotic interface. (a) The human and the interrogator held the stylus of a haptic device. Position information was transmitted between the two devices and forces were applied on each of the devices according to the particular handshake (modified with permission from [5]). (b) Block diagram of the experimental system architecture. The different models and the noise were substituted in the "computer" block. The human received a force proportional, by the factor K_t, to the difference between the positions of the interrogator—$x_{inter}(t)$—and the human—$x_{human}(t)$. $G_h >$ and G_c are the gains of the human and the computer force functions, respectively, that control the force applied to the interrogator. When an interrogator interacted with a handshake model, as far as the interrogator was concerned, the block diagram was reduced to the part that is encapsulated by the dashed frame by setting $G_h = 0$ and $G_c = 1$. (c) Closeup view of the hand-device interface.

roles in the interaction and generated handshakes by imitating the interrogator's previous movements; 2) the λ model, which takes into account physiological and biomechanical aspects of handshake; and 3) the iML-Shake model, which uses a machine learning approach to reconstruct a handshake. Each of these models is based on a different aspect of human sensorimotor control. Therefore, we did not have an a priori hypothesis as to which of the models would be more human-like, and the study was exploratory in its nature. In the discussion section, we highlight the similarities and differences of the models.

2 The Turing-Like Handshake Test

Following the original concept of the classical Turing test, each experiment consisted of three entities: ***human***,

computer, and ***interrogator***. These three entities were interconnected via two Phantom Desktop haptic devices and a teleoperation channel (see Fig. 2). Two human performers participated in each experiment: ***human*** and ***interrogator***. Throughout the test, each of the participants held the stylus of one haptic device and generated handshake movements. The participants' vision of each other's hand was occluded by a screen (Fig. 2a).

The ***computer*** employed a simulated handshake model that generated a force signal as a function of time, the 1D position of the interrogator's haptic device, and its temporal evolution. This force was applied on the haptic device that the interrogator held. In the remainder of the paper, we use the following notation for forces: F_a is the force applied **by** or **according to** element a, and f_a is the force applied **on** element a. Hence, the force applied by the model, in the most general notation, was

$$F_{\text{model}}(t) = \Phi[x_{inter}(t), t] \quad 0 < t \leq T_h, \tag{1}$$

where $\Phi[x_{inter}(t), t]$ stands for any causal operator, T_h is the duration of the handshake and $x_{inter}(t)$ are the positions of the interrogator's haptic device up to time t.

In each trial, both haptic devices applied forces on the human and the interrogator, according to the general architecture that is depicted in Fig. 2b. The human was presented with a teleoperated handshake of the interrogator. In our implementation, it was a force proportional to the difference between the positions of the interrogator and of the human. The interrogator was presented with two consecutive handshakes. In one of the handshakes—the ***standard***—the interrogator interacted with a computer handshake model (Fig. 1a), namely

$$f_{\text{inter}}(t) = F_{\text{model}}(t). \tag{2}$$

The other handshake—the ***comparison***—is a handshake that is generated from a linear combination of the human handshake and noise (Fig. 1c) according to

$$f_{\text{inter}}(t) = \beta \cdot F_{\text{noise}}(t) + (1 - \beta) \cdot F_{\text{human}}(t), \tag{3}$$

where $F_{\text{human}}(t)$ is, ideally, the force applied by the human, and in our implementation, a force calculated based on the difference between the positions of the human and the interrogator; $F_{\text{noise}}(t)$ is a signal that was intended to distort the human-likeness of the human handshake; β was one of n_r equally distributed values in the range between 0 and 1, e.g., {0, 0.2, 0.4, 0.6, 0.8, 1}. According to (3), when β was set to 0, the force applied on the interrogator was generated fully by the human; when it was set to 1, the interrogator felt a force that was generated solely according to $F_{\text{noise}}(t)$. $F_{\text{noise}}(t)$ was chosen such that when presented alone, it was perceived to be as little human-like as possible. This allowed effective comparison of a simulated handshake with a human handshake corrupted by different levels of noise. The idea is that if more noise is required to degrade the human handshake such that it becomes indistinguishable from the model, then the model is less human-like. Such an approach was suggested in the context of assessing virtual environments according to the amount of noise required to degrade the real and virtual stimulation until the perceived environments become indistinguishable [43], [44]. In the current study, we chose the noise as a mixture of sine functions with frequencies above the natural bandwidth of the human handshake [4], [5], [45] and within the bandwidth of physiological motor noise, but the general framework is flexible, and any other function can be used instead, as long as it is not human-like.

Each trial of the Turing-like test consisted of two handshakes, and the interrogator was asked to compare between the handshakes and answer which one felt more human-like.

3 The Three Models for Handshake

In this section, we describe each of the models for human handshake examined in the current study. We will start by describing the physical interaction of the interrogator with the haptic device when he/she is introduced to a model, as in (2). In this case, as far as the interrogator is concerned, the block diagram in Fig. 2b is reduced to the part that is encapsulated by the dashed frame by setting $G_h = 0$ and $G_c = 1$.

A similar architecture of interaction with a haptic device was used in numerous classical studies in the field of sensorimotor control [32], [34], [35], [38], [39], [40], [41], [42], [46]. Typically in these studies, an external perturbation is applied to the hand using a haptic device, and then, a computational model of the movement is constructed and can be tested in a simulation. In such simulation, the computational model replaces the hand and results in movement trajectories that are similar to the experimental trajectories. Generally, this yields differential equations in the form of [34]

$$D(x, \dot{x}, \ddot{x}) + E(x, \dot{x}, \ddot{x}) = C(x, \dot{x}, t), \tag{4}$$

where $D(x, \dot{x}, \ddot{x})$ represents the passive system dynamics (hand and haptic device), $E(x, \dot{x}, \ddot{x})$ represents the environment dynamics—the active forces applied by the haptic device, and $C(x, \dot{x}, t)$ represents the forces that depend on the operation of the controller and are actively applied by the muscles. This equation is solved numerically and yields the simulated trajectories.

In our implementation, an equation similar to (4) can be written, but the interrogator hand and the haptic device switch roles. The dynamic equation that describes the system is

$$D(x, \dot{x}, \ddot{x}) + F_{\text{inter}}(t) = F_{\text{model}}(t), \tag{5}$$

where $D(x, \dot{x}, \ddot{x})$ is the passive system dynamics (interrogator hand and haptic device), $F_{\text{inter}}(t)$ is the force applied by the interrogator and $F_{\text{model}}(t)$ is the force that models the forces that would be applied by the human hand in a human handshake, and is actually applied by the haptic device. Note, that $F_{\text{inter}}(t)$ replaces $E(x, \dot{x}, \ddot{x})$ from (4), and $F_{\text{model}}(t)$ replaces $C(x, \dot{x}, t)$ from (4). More importantly, while (4) represents a computational model, (5) describes a physical interaction, and its only computed part is $F_{\text{model}}(t)$.

3.1 Tit-for-Tat Model

In the early 80s, Axelrod and Hamilton examined different strategies for optimizing success in the Prisoner's Dilemma

game [47]. The proposed strategies were competed against each other in a tournament that revealed that the best strategy is when the players imitate each other's actions from the previous iteration. The following algorithm employs a similar strategy, and thus, it has been given the same name "Tit-for-Tat."

This model is based on the assumption that during a single handshake, the behavior of each participant can be characterized as one of two possible roles—a leader or a follower—and that the decision on which role to take requires a perception of the other party's choice [15]. In addition, we assume that this approximation does not change during a single handshake.

When designing this model, we considered the cyclic property of the handshake movement. A cycle of a movement was defined by the zero-crossing point in the vertical axis. This zero point is set for every handshake as the starting position of the interrogator's device at the moment the handshake began. Initially, the tit-for-tat algorithm waited for $750\ \mathrm{ms}$ to see if the interrogator would initiate the handshake as a leader. If the interrogator made a displacement of $30\ \mathrm{mm}$ or more, the tit-for-tat algorithm acted as a follower, and imitated the handshake of the leader. During the first cycle of a movement (up until the second zero position crossing point in the position trace), $T_{FirstCycle}$, no forces were applied to the handle by the algorithm. The acceleration of the interrogator was recorded for the first movement cycle of the current handshake, $a_h(t)$. For all subsequent cycles, the algorithm generated forces that would be required to produce the same trajectory in the unloaded Phantom handle. These forces were determined by the recorded acceleration during the first cycle of the handshake, $a_h(t)$, multiplied by a constant k. We set the value of k so that the generated force would produce a movement with similar position amplitude generated by interrogators when performing handshake movements through the telerobotic system. The forces started to be activated at the moment the hand was at the same position as it was at time 0.

$$\text{If } |\mathrm{x_{inter}(t)} - \mathrm{x_{inter}(0)}| > 30\ \mathrm{mm} \text{ for at least one } \mathrm{t_i}|\mathrm{t_i} < 750\ \mathrm{ms}:$$
$$F_{\text{model-}follower}(t) = \begin{cases} 0 & 0 < t \le T_{FirstCycle}, \\ k \cdot a_h(t) & T_{FirstCycle} < t \le T_h, \end{cases} \tag{6}$$

where $a_h(t) = \ddot{x}_{\mathrm{inter}}(t \bmod T_{FirstCycle})$, and "mod" stands for the modulo operation (the remainder of division). If the interrogator did not initiate a movement larger than $30\ \mathrm{mm}$ within the first $750\ \mathrm{ms}$ of the handshake, the model took over the leader rule. In this case, the forces were determined by the recorded acceleration during the first cycle of the last handshake in which this model was presented, $a_{h-1}(t)$, multiplied by the constant k.

$$\text{If } |\mathrm{x_{inter}(t)} - \mathrm{x_{inter}(0)}| < 30\ \mathrm{mm} \text{ for all } \mathrm{t_i}|\mathrm{t_i} < 750\ \mathrm{ms}:$$
$$F_{\text{model-}leader}(t) = \begin{cases} 0 & 0 < t \le 750\ \mathrm{ms} \\ k \cdot a_{h-1}(t) & 750\ \mathrm{ms} < t \le T_h, \end{cases} \tag{7}$$

where $a_{h-1}(t) = \ddot{x}^*_{\mathrm{inter}}(t \bmod T^*_{FirstCycle})$; "*" stands for previous trial.

In the beginning of the experiment, we familiarized the interrogator with trials containing examples of all the possible handshakes that he/she was expected to meet during the experiment. The answers of the interrogator from these trials were not analyzed (see Section 4). In these trials, we asked the interrogators to be active in the handshake; thus, we were able to collect data for a template for the tit-for-tat algorithm in case it needed to act as the leader in the first test with the interrogator. This also creates a difference between the data use of the algorithms. The tit-for-tat model used data from previous interactions in the same performer-interrogator pairing, while the other models did not.

3.2 λ Model

The idea of threshold control in the motor system, and specifically for hand movements, was proposed in the sixties by Feldman [48]. According to this hypothesis, for every intentional movement, there is a virtual position of the arm that precedes its actual position so that forces emerge in the muscles depending on the differences between the two positions and velocities. This virtual position is named "a threshold position" [49]. We designed the λ model for human handshake by assuming that during a handshake the hand follows an alternating threshold position. The smooth movements of the handshake emerge from taking into account the physiology and biomechanics of muscle activation.

A movement of a limb involves activations of two groups of muscles: flexor and extensor. For a movement around the elbow axis, when the elbow angle (θ) increases, the flexor group of muscles is defined here as the ones that lengthen, and the extensor group are the ones that shorten. For simplicity, we assume that the movement is around a single joint (elbow), and that the two muscle groups, flexor, and extensor, are symmetric.

According to the model, muscle forces and joint torques emerge as a result of two types of motor commands. One command, R, specifies the desired angle position of the joint, in which the flexor and extensor muscle groups may both be silent. The second command, C, determines the positional range ($2C$) in which the two muscle groups are coactivated. These commands define an individual muscle threshold (λ) for each muscle group

$$\lambda_f = R - C, \tag{8}$$

$$\lambda_e = R + C. \tag{9}$$

Here, and in all the equations below, the subscripts f and e indicate that the associated variable is related to the flexor and the extensor muscle groups, respectively. This model takes into account that under dynamic conditions the threshold muscle length (λ^*) is a decreasing function of velocity due to the dynamic sensitivity of afferent feedback to the motor neurons [50]

$$\lambda^* = \lambda - \mu \cdot \omega, \tag{10}$$

where ω is the angular velocity and μ is a constant with the value $80\ \mathrm{ms}$ [49]. The only difference between the dynamic threshold between the flexor and extensor muscle groups is expressed by the individual muscle threshold (λ) differences as described in (8) and (9).

The magnitude of muscle activation (A) at time t depends on the current joint angle (θ) and its distance from the desired position at the same moment (the dynamic threshold λ^*), as presented in (11) and (12)

$$A_f = [\theta - \lambda_f^*]^+, \tag{11}$$

$$A_e = [\lambda_e^* - \theta]^+. \tag{12}$$

Following the passive properties of the muscle (elasticity and damping), the total force developed by the muscles (M) depends on the current joint angle and the threshold position at the same moment. The following equations define these invariant torque-angle characteristics [48]

$$M_f(A_f) = -a \cdot (e^{\alpha \cdot A_f} - 1), \tag{13}$$

$$M_e(A_e) = a \cdot (e^{\alpha \cdot A_e} - 1), \tag{14}$$

where $a = 1.2\,\mathrm{Nm}$ and $\alpha = 0.05\ \mathrm{deg}^{-1}$ [49] are constants that determine the magnitude and shape of the joint invariant torque-angle characteristics profile, respectively [51]. The opposite signs between the expressions in (13) and (14) reflect the opposing torque directions generated by the flexor and extensor muscle groups.

In addition to its dependency on length, the muscle torque is affected by the changing velocity of the muscle fibers, as denoted by (15). In this equation, the torque, T_f, is presented for the flexor muscles group; thus, positive velocity of the joint is related to muscle lengthening, and vice versa. A similar formula can be written for the extensor muscle torque, T_e, by taking into account that this group of muscles shortens when the velocity of the joint is positive.

The torque generated by the flexor muscle is

$$T_f = \begin{cases} 0, & \omega \le -V_m \\ \dfrac{M_f(1+\frac{\omega}{V_m})}{1-\frac{\omega}{b}}, & -V_m \le \omega < 0;\ b' = \dfrac{0.3 \cdot b \cdot V_m}{b - V_m} \\ \dfrac{M_f(1-\frac{1.3\omega}{b'})}{1-\frac{\omega}{b'}}, & \omega > 0, \end{cases} \tag{15}$$

This equation is formulated based on previous studies that analyzed the velocity-dependent force generation of muscle. When the muscle contracts, torque is generated according to the relation proposed in Hill's model [52]. While stretching, the muscle torque rises with increasing velocity until it saturates at a value exceeding the muscle static torque value by a factor of $1.1 - 1.5$ [53].

All the values of the constant parameters in the model were set to match experimental movements: $M_f = 1.3$, $b = 80\,\mathrm{deg}/s$, and $V_m = 200\,\mathrm{deg}/s$. The R and C commands were ramp shaped, with a ramp velocity of $v = 100\,\mathrm{deg}/s$ and $v = 10\,\mathrm{deg}/s$, respectively. For the purpose of implementing the model with the Phantom haptic device, we transformed all the relevant outputs of the model from units of degrees (in elbow joint coordinates) to meters (hand end-point coordinates). To perform this transformation, we calculated the average forearm length and its standard deviation (315.8 ± 27.8 mm) of 52 young adults (ages 18-36). Therefore, assuming small angular movements, we set $\Delta x[mm] = 300[mm/rad] \cdot \Delta\theta[rad]$ where Δx is the hand end-point displacement and $\Delta\theta$ is the joint angle displacement.

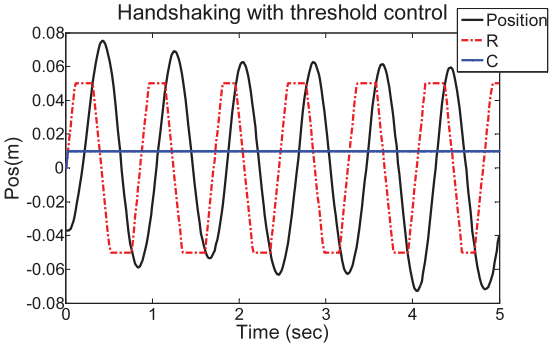

Fig. 3. An example of one handshake of the interrogator with the threshold control model. position (solid black line) following activation of the cooperative commands R (dashed-dotted red lines) and C (solid blue line). The figure presents the commands after transformation from degrees to meters, with the R command amplitude value of ~ 5 cm (10 degree), and the C command value of $\sim$1 cm (2 degree).

To determine the plateau boundaries value of the R command (Fig. 3) which sets the desired angle trajectory during the 5 s lasting handshake, we measured the end-point positional amplitudes (the absolute difference between sequential maxima and minima in the position trace) of subjects while they generated handshake movements through the telerobotic system. We found an average end-point positional amplitude of 100 ± 30 mm [4]. Thus, we used angular positional amplitude of $20\,\mathrm{deg}$.

We assumed that when the interrogators hold the Phantom device, their initial elbow angle is $R_0 = 90\,\mathrm{deg}$. Thus, we set the minimum and maximum values of R to be $R_{up} = 80\,\mathrm{deg}$ and $R_{down} = 100\,\mathrm{deg}$, respectively. From its initial position, the value of R decreased first to the desired position R_{up} so that the movement direction in the beginning of the handshake would be upward [54]. Each switch of the R command from one plateau state to another (up down or down up) occurred when the elbow angle of the interrogator approached the value of the relevant extremum value of R (R_{up} when θ decreased and R_{down} when θ increased) by 10 percent.

The forces applied by the Phantom device on the interrogator were generated according to the online computed torque

$$F_{\mathrm{model}} = c \cdot (T_f + T_e), \tag{16}$$

where c is a unit conversion constant from muscle torques to simulated handshake forces.

In terms of data use, the λ model, unlike the other models, uses only instantaneous position of the interrogator to calculate the forces in (16). However, some information about general human movements and handshakes was incorporated when the specific parameters values were chosen.

3.3 iML-Shake Model

The iML-Shake model is a simple implementation of machine learning. The underlying idea is that human behavior can be seen as an input-output function: subjects observe positions and produce forces. If enough data from human subjects were available, such machine learning

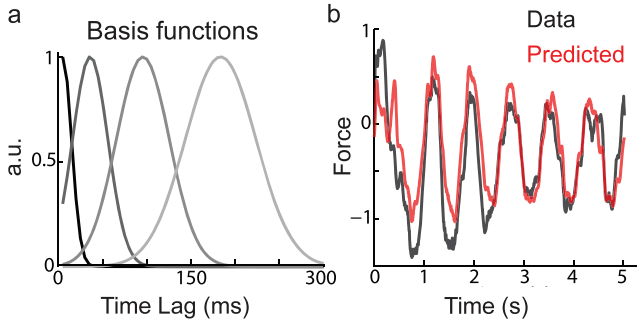

Fig. 4. Basis functions of the general linear model and handshake simulation according to the iML-Shake. (a) Truncated Gaussian temporal basis functions used in the iML-Shake algorithm, in arbitrary units (a.u.). (b) Force data (black line) from one trial and fittings of the model (red line).

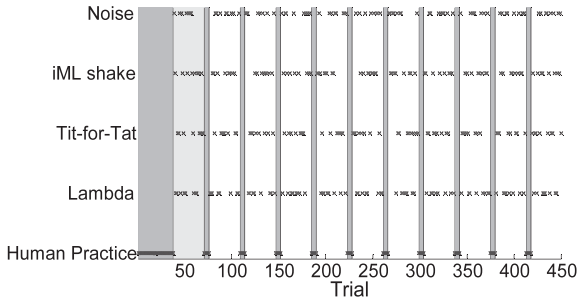

Fig. 5. Experimental trials order. Each trial included a human handshake and additional handshake as specified in the figure. Dark-gray shaded areas are human practice trials. Namely, both handshakes were human. Light-gray shaded area is one training block; the answers in these blocks were not analyzed.

systems should be able to approximate any possible handshake behavior humans could ever produce. Here, we present a simple linear version of this machine learning strategy.

In the iML-Shake, the output force was a linear combination of time t and each of the state variables (position $x_{\text{inter}}(t)$, estimated velocity $v(t)$ and estimated acceleration $a(t)$) convolved with a set of 4 truncated Gaussian temporal basis functions (Fig. 4a) [55]. Velocity and acceleration were estimated from the interrogator's position as

$$v(t) = \frac{x_{\text{inter}}(t) - x_{\text{inter}}(t - \Delta t)}{\Delta t}, \tag{17}$$

$$a(t) = \frac{v(t) - v(t - \Delta t)}{\Delta t}. \tag{18}$$

The 14 parameters—corresponding to baseline, time, and 12 covariates that result from the convolution of the state variables with the temporal filters—were fitted using linear regression to 60 trials of training data from one training subject, collected before the experiments started. No additional data were used to adapt the regression while the test was performed. We then calculated $F_{\text{model}}(t)$ as a linear function of the covariates with added independent and normally distributed noise

$$F_{\text{model}}(t) = \Psi(t) \cdot \beta + \varepsilon(t), \quad \varepsilon(t) \sim N(0, \sigma^2), \tag{19}$$

where β is the column vector of parameters and $\Psi(t)$ is a 14D row vector that contains the values of the covariates at time t. The training data were interpolated to match a sampling rate of 60 Hz and we used cross validation to control for overfitting.

In terms of data usage, the iML-Shake model used the position of the interrogator within the specific handshake, as well as past experience. However, unlike in the tit-for-tat model, the past experience was collected before the experiments started. Hence, no specific human interrogator pairing information was used.

4 Methods

4.1 Experimental Procedure, Apparatus, and Architecture

Twenty adults (ages 23-30) participated in the experiment after signing the informed consent form as stipulated by the Institutional Helsinki Committee, Beer-Sheva, Israel. In each experiment, two naïve performers—human and interrogator—controlled the stylus of a Phantom (R) Desktop haptic device (SensAble Technologies) and generated handshake movements, as depicted in Fig. 2. During the handshake the participants' vision of each other's hand was occluded by a screen that was placed between them (Fig. 2a). The duration of each handshake was 5 s (T_h in (1)). Throughout the entire experiment, the interrogator was asked to follow the instructions presented on a screen that both the interrogator and the human subject where able to see (Fig. 2a). The interrogator initiated the handshake by pressing a specific key on the keyboard. When the key was pressed the word "HANDSHAKE" appeared on the screen. This way, the interrogator signaled the initiation of a handshake to the human. Throughout the experiment, the interrogator was requested to answer which of the two handshakes within a single trial felt more human-like by pressing the appropriate key on the keyboard. Both haptic devices were connected to a Dell Precision 450 computer with dual CPU Intel Xeon 2.4 GHz processor. The position of the interrogator, $x_{\text{inter}}(t)$, and of the human, $x_{\text{human}}(t)$, along the vertical direction were recorded at a sampling rate of 1,000 Hz. These position signals were used to calculate the forces that were applied by each of the devices according to the overall system architecture depicted in Fig. 2b. The human performer always felt a force that was proportional to the difference between the positions of the interrogator and the human himself, namely

$$f_{\text{human}}(t) = K_t \cdot (x_{\text{inter}}(t) - x_{\text{human}}(t)), \tag{20}$$

where $K_t = 150N/m$. The interrogator felt one of two possible forces. The first option was a combination of the force in (20) and noise generated by the computer, namely

$$f_{\text{inter}} = G_h \cdot K_t \cdot (x_{\text{human}}(t) - x_{\text{inter}}(t)) + G_c \cdot F_{\text{computer}}(t); \quad F_{\text{computer}}(t) = F_{\text{noise}}(t) \tag{21}$$

where G_h and G_c are the gains of the human and computer force functions. The second option was a computer-generated force according to each of the models that were described in Section 3, namely

$$f_{\text{inter}} = F_{\text{computer}}(t); \quad F_{\text{computer}}(t) = F_{\text{model}}(t). \tag{22}$$

The calculation of $F_{\text{computer}}(t)$ was performed at 60 Hz, and the force was interpolated and rendered at 1,000 Hz.

The timeline of the experiment is presented in Fig. 5. Each experiment started with 38 practice trials (76 handshakes) in which the interrogator shook hands only with the human through the telerobotic system, namely $G_h = 1$ and $G_c = 0$. The purpose of these practice trials was to allow the participants to be acquainted with a human handshake in our telerobotic system, and also, to provide starting information to the tit-for-tat algorithm.

In each trial, the interrogator was presented with a pure computer handshake, namely $G_h = 0$ and $G_c = 1$, which was one of the three candidate models described in Section 3, and a human handshake combined with noise, namely $G_h = 1 - \beta$ and $G_c = \beta$. β was assigned with eight equally distributed values from 0 to 1: $\beta = \{0, 0.142, 0.284, 0.426, 0.568, 0.710, 0.852, 1\}$. The noise function was chosen as a mixture of sine functions with frequencies above the natural bandwidth of the human handshake [4], [5], [45]:

$$f(t) = \sum_{i=1}^{5} 0.7 \cdot \sin(2\pi\omega_i t); \quad \omega_i \sim U(2.5 \text{ Hz}, 3.5 \text{ Hz}), \qquad (23)$$

where U(a,b) is a continuous uniform distribution between a and b.

Within each block, there were eight calibration trials in which the combined human-noise handshake with $G_h = 1 - \beta$ and $G_c = \beta$, for each of the eight values of β, was compared to a combined human-noise handshake with $G_h = 0.5$ and $G_c = 0.5$. In these trials, one of the handshakes was always composed of a greater weight of human forces than the other handshake. We assume that a handshake with larger weight of human versus noise is perceived as more human, and therefore, the participant should be able identify the handshake that is more similar to that of a human. Thus, the purpose of these trials was to verify that the interrogators were attending to the task and that they were able to discriminate properly between handshakes with different combinations of human generated force and noise.

Overall, each experimental block consisted of 32 trials: each of the eight linear combinations of noise and human performance were compared with each of the three models as well as with the noise combined with human performance (calibration trials). The order of the trials within each block was random and predetermined. Each experiment consisted of 10 blocks. Thus, each of the models was presented to the interrogator in 80 handshakes. One experimental block (32 trials) was added at the beginning of the experiment for general acquaintance with the system and the task. The answers of the interrogators in this block were not analyzed. To preserve the memory of the feeling of a human handshake in the telerobotic setup, the subject was presented with 12 human handshakes after each experimental block. It is important to note that this allows interrogators not only to detect human-like handshakes but also to detect the specific aspects of their current partner. As such, a human may, on average, be technically worse than human-like. To increase the motivation of the participants, at the end of each block, they received a grade that was computed based on their answers in the calibration trials. For example, an answer in a calibration trial was considered correct when the interrogator stated that a handshake that contained 0.852 human generated force and 0.148 noise was more human-like than a handshake that contained 0.5 human generated force and 0.5 noise.

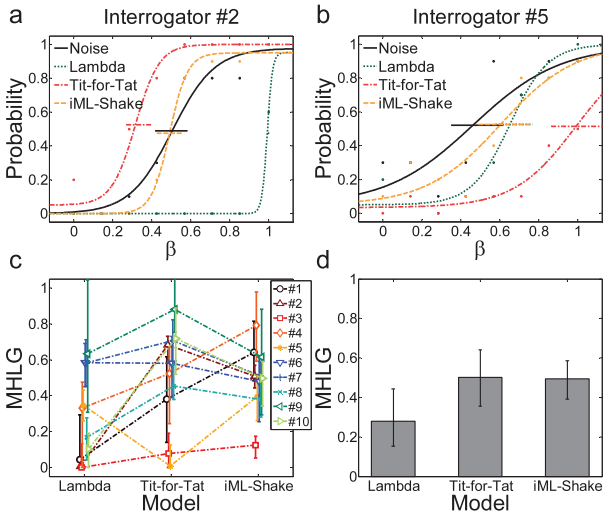

Fig. 6. Human likeness for the models. Panels (a) and (b) present examples of psychometric curves that were fitted to the answers of interrogator #2 and interrogator #5, respectively. Dots are data points, and the horizontal bars are 95 percent confidence intervals for the estimation of PSE. A model with higher *MHLG* yields a curve that is shifted further to the left. (c) The *MHLGs* that were calculated according to each of the 10 interrogators who performed the test. Symbols are estimations of *MHLG*, and vertical bars are 95 percent confidence intervals. (d) Means with bootstrap 95 percent confidence intervals (error bars) that were estimated for each of the models using the *MHLG* of all the interrogators.

4.2 The Model Human-Likeness Grade

To assess the human likeness of each model, we fitted a psychometric curve [56], [57] to the probability of the interrogator to answer that a stimulus handshake is more human-like than a reference as a function of β—the relative weight of noise in the comparison handshake. In accordance with our assumption that a higher weight of the noise component in the comparison handshake yields higher probability to choose the standard handshake as more human-like, this probability approaches one as β approaches one, and zero when it approaches zero. In general, such psychometric curves are sigmoid functions [56], [57], and they can reveal both the bias and uncertainty in discriminating between the standard and the comparison handshakes (Figs. 6a and 6b). The bias in perception, or more specifically, the point of subjective equality (PSE), can be extracted from the 0.5 threshold level of the psychometric curve, indicating the value of β for which the standard and the comparison handshakes are perceived to be equally human-like. Namely, for a model that is indistinguishable from a human, the expected PSE is 0 if humans make no systematic mistakes or "slips" in their judgments. Similarly, for a model that is as human-like as the noise function (hence, the least human-like model) the expected PSE is 1, again assuming no systematic mistakes or slips. We subtracted the value of PSE from one to obtain the $MHLG$ (24), such that $MHLG = 0$ means that the model is clearly nonhuman like, and $MHLG = 1$ means that the tested model is indistinguishable from the human handshake.

$$MHLG = 1 - \mathrm{PSE}, \tag{24}$$

The models that are perceived as least or most human-like possible yield $MHLG$ values of 0 or 1, respectively. Therefore, $MHLG$ is cut-off at 0 and 1.

We used the Psignifit toolbox version 2.5.6 for Matlab (available at http://www.bootstrapsoftware.org/psignifit/) to fit a logistic psychometric function [57] to the answers of the interrogators, extracted the PSE, and calculated the $MHLG$ of each of the models according to (24).

4.3 Statistical Analysis

We used 1-way ANOVA with repeated measures in order to determine whether the difference between the $MHLG$ values of the models was statistically significant. We used the Tukey's honestly significant difference criterion ($\mathrm{p} < 0.05$) to perform the post-hoc comparisons between the individual models. We performed this statistical analysis using Matlab statistics toolbox.

5 Results

Examples of psychometric curves that were fitted to the answers of two selected interrogators are depicted in Fig. 6a and 6b. The $MHLG$ of individual subjects for each of the Turing-like tests are presented in Fig. 6c. These figures reveal substantial differences of opinion among the interrogators. For example, interrogator #2 (Fig. 6a) perceived the λ model as the least human-like (dotted curves), while the tit-for-tat model was perceived as the most human-like (dashed-dotted curves), as opposed to interrogator #5 (Fig. 6b) who perceived the tit-for-tat model as the least human-like, and yielded higher $MHLG$ for the λ and iML-Shake (dashed curves) models. The calibration curves (noise model, solid curves) indeed yielded a PSE that was not statistically significantly different from 0.5. Furthermore, for a few interrogators, we did not observe significant differences between the $MHLG$ of all three models. Estimations of the mean $MHLG$ of all models across interrogators are presented in Fig. 6d, together with the 95 percent confidence intervals for these estimations. There was a statistically significant difference between the $MHLG$ values of the three models (1-way ANOVA with repeated measures, $F_{2,18} = 4.57, p = 0.0248$). The tit-for-tat and iML-Shake models yielded statistically significantly higher $MHLG$ values than the λ model (Tukey's honestly significant difference criterion, $\mathrm{p} < 0.05$), respectively. There was no statistically significant difference between the $MHLG$ of the tit-for-tat and the iML-Shake models.

6 Discussion

In this study, we presented three models for human handshake: λ, based on physiological and biomechanical aspects; tit-for-tat, based on leader-follower roles and imitation; and iML-Shake, based on machine learning. The tit-for-tat and the iML-Shake models were perceived statistically significantly more human-like than the λ model, but not significantly different between them. However, the grading was not consistent among subjects.

6.1 Further Development of the Models

Each of the models that were presented in this paper has its own strength, but each could be improved. Moreover, the best features of each could be combined into one handshake to improve the human likeness.

In the passive phases of the tit-for-tat algorithm, the interrogator experiences zero forces, while in reality a "passive hand" would present inertial and perhaps some viscoelastic impedance. The algorithm could start to modify its behavior after a typical voluntary reaction time, and reduce its impedance as the interrogator's intentions became apparent. This would require a more accurate model of the relevant musculoskeletal structures and their intrinsic mechanical properties, some of which are captured in the λ model. Such models are easily constructed in the MSMS environment (MusculoSkeletal Modeling Software, available from http://mddf.usc.edu; [58]), but are out of the scope of the current work. However, initial values for such properties could be taken from the literature, e.g., $\mathrm{M} = 0.15$ kg, $\mathrm{B} = 5$ Ns/m, and $\mathrm{K} = 500$ N/m for wrist movements [59], or $\mathrm{M} = 1.52$ kg, $\mathrm{B} = 66$ Ns/m, $\mathrm{K} = 415$ N/m for elbow movements [34].

A unique aspect of the tit-for-tat model is the notion of two roles in a sensorimotor interaction: a leader and a follower. The model adjusts itself to the interrogator by taking one of these roles. However, the limitation here is that the model can take the role of a leader only if it was introduced at least once with a leader interrogator.

The λ model generates handshakes according to the threshold control hypothesis. It can be improved by changing the threshold position whenever a change in movement direction is detected. In addition, the implementation of the λ model included some simplifications (e.g., neglecting the inertia of the arm and assuming one joint and two muscles), and it is not adaptive, namely, we set the movement range to specific fixed values, while different interrogators may display movements with different amplitudes.

Unlike the other two models, the λ model takes into account dynamical properties that have previously been demonstrated to fit the biomechanical characteristics of the hand. These include the invariant characteristics of the passive force generated by the muscle, and the force-velocity relationship of the muscles.

The iML-Shake is based on linear regression. This approach represents a large class of stateless and time invariant methods. We could allow smoother predictions and recovery from input failures by utilizing another class of state-space algorithms that models time variations [55, Section 13.3]. The advantage of this approach is that by making minimal assumptions about the mapping between the inputs and outputs of the handshake "function," we are factoring in many details of human handshake biomechanics that may be unknown, difficult to quantify, or inefficient to implement.

Further improvement can be achieved by including additional knowledge about human cognitive and biomechanical characteristics in a more specific machine learning approach. For example, for the mechanics we could include the state-space evolution of multilink serial chains as a model of the arm and hand, with contact forces and torques [60]. For behavioral strategies, we could include the evolution of beliefs about the other's motor plan and combine it with our agent's goals. We can formulate this problem as the inversion of a Partially Observable Markov Decision Process (POMDP), which has been shown to resemble how humans think about others' intentions [61].

6.2 Subjectivity versus Objectivity

The difference in grading among interrogators limits conclusions about the relative performance of the algorithms (see Figs. 6a, 6b, and 6c). A possible explanation is that the internal representation of human-likeness is multidimensional, and each interrogator might follow a different decision path in the space of human likeness features [7]. According to this view, all the interrogators would correctly identify the least and the most human-like possible handshakes, but may have various opinions about the salient feature characterizing human-likeness. Moreover, humans themselves exhibit a great range of handshake styles, both as individuals and as members of ethnic and national cultures. Thus, the test results could be biased by similarities between the handshake style of the interrogator and of the robotic algorithm, or by dissimilarities between the interrogator and the human handshake to which the robot is being compared. The original Turing test for artificial intelligence has a similar cultural problem. In future studies, a larger number of subjects could be tested in a fully factored design to make sure that all combinations of interrogators, robots, and human performer are tested against each other so that such trends could be extracted statistically from the results. Such test results might provide quantitative insights into cultural differences among humans [62], [63].

The difference in grading might be the result of the subjective and declarative nature of the test, so it may be useful to look at objective, physiologically related, measures, such as skin conductance response [64], heart rate [65], postural responses [66], or task performance [20], [67], [68]. This is of special importance in the light of evidence that declarative perception is not always consistent with motor responses [69], [70], [71], [72], [73].

6.3 Future Turing-Like Handshake Tests

For this preliminary investigation, we limited the handshake dynamics to those that can be generated in one axis via a Phantom handle. A great deal of information is conveyed in other dimensions of the human handshake, such as distribution of grip forces among the fingers and off-axis motions of the wrist and forearm. The rapid improvements in anthropomorphic robotic hands and arms (e.g., Shadow Robot [74] and DLR-HIT [75]) should make it feasible to create much more realistic handshake Turing tests. However, these will require much more complex control algorithms.

The comparison of the three models may not be entirely fair, and future versions of the handshake Turing test may be adapted toward this aim. Specifically, the tit-for-tat strategy uses data about the specific interrogator-subject pairing. This problem is compounded by the fact that there are human-human reminder trials in which a subject can learn about the specific characteristics of their partner handshakes. Both the tit-for-tat and iML-Shake models use past data, while the λ model only uses instantaneous information about the interrogator movements. The λ and iML-Shake models both use the information of the whole 5 s of the handshake, while the tit-for-tat model only uses the first cycle of movement. To take into account these differences, in future studies, only models that use similar data should be compared to each other and a quantitative measure of model complexity could be developed and incorporated into the $MHLG$.

It may also be important to let each interrogator experience sequential trials with the same algorithm interspersed randomly with the same human. This would be more akin to the extended dialogue of the original Turing test, in which the interrogator uses the results of one query to frame a subsequent query.

Ultimately, a haptically enabled robot should itself have the ability to characterize and identify the agents with which it interacts. This ability fulfills the purpose of a human handshake. Thus, the robotic Turing test presented here could be made bidirectional, testing the ability of the robot to perceive whether it is shaking hands with a human or with another robotic algorithm—the reverse handshake hypothesis [8]. According to this hypothesis, once a model that best mimics the human handshake is constructed, it itself can then be used to probe handshakes. Such an optimal discriminator might require enhancements of sensory modalities such as tactile perception of force vectors, slip, or warmth [76].

6.4 Concluding Remarks

We assert that understanding the sensorimotor control system is a necessary condition for understanding brain function, and it could be demonstrated by building a humanoid robot that is indistinguishable from a human. The current study focuses on handshakes via a telerobotic system. By ranking models that are based on the prevailing scientific hypotheses about the nature of human movement, we should be able to extract salient properties of human sensorimotor control, or at least the salient properties required to build an artificial appendage that is indistinguishable from a human arm.

Beyond the scientific insights into sensorimotor control, understanding the characteristic properties of healthy hand movements can be very helpful for clinical and industrial applications. For example, it may facilitate an automatic discrimination between healthy hand movements and movements that are generated by motorically impaired individuals, such as cerebral palsy patients [77], [78] and Parkinson patients [79]. In future industrial and domestic applications, robotic devices are expected to work closely and interact naturally with humans. Characterizing the properties of a human-like handshake is a first step in that direction.

Acknowledgments

The authors wish to thank Prof. Anatol Feldman for his assistance in constructing the λ model, and Mr. Amit Milstein and Mr. Ofir Nachum for their help in implementing the models and the experiments. This work was supported by the Israel Science Foundation Grant number 1018/08. I. Nisky was supported by the Kreitman and Clore Foundations.

References

[1] W.F. Chaplin, J.B. Phillips, J.D. Brown, N.R. Clanton, and J.L. Stein, "Handshaking, Gender, Personality, and First Impressions," *J. Personality and Social Psychology*, vol. 79, no. 1, pp. 110-117, 2000.

[2] G.L. Stewart, S.L. Dustin, M.R. Barrick, and T.C. Darnold, "Exploring the Handshake in Employment Interviews," *J. Applied Psychology*, vol. 93, no. 5, pp. 1139-1146, 2008.

[3] A.M. Turing, "Computing Machinery and Intelligence," *Mind, a Quarterly Rev. of Psychology and Philosophy,* vol. LIX, no. 236, 1950.

[4] G. Avraham, S. Levy-Tzedek, and A. Karniel, "Exploring the Rhythmic Nature of Handshake Movement and a Turing-Like Test," *Proc. Fifth Computational Motor Control Workshop,* 2009.

[5] A. Karniel, G. Avraham, B.-C. Peles, S. Levy-Tzedek, and I. Nisky, "One Dimensional Turing-Like Handshake Test for Motor Intelligence," *J. Visualized Experiments,* vol. 46, p. e2492, 2010.

[6] G. Avraham, I. Nisky, and A. Karniel, "When Robots Become Humans: A Turing-Like Handshake Test," *Proc. Seventh Computational Motor Control Wokshop,* 2011.

[7] I. Nisky, G. Avraham, and A. Karniel, "Three Alternatives to Measure the Human Likeness of a Handshake Model in a Turing-like Test," *Presence,* vol. 21, no. 2, pp. 156-182, 2012.

[8] A. Karniel, I. Nisky, G. Avraham, B.-C. Peles, and S. Levy-Tzedek, "A Turing-Like Handshake Test for Motor Intelligence," *Proc. Int'l Conf. Haptics: Generating and Perceiving Tangible Sensations,* pp. 197-204, 2010.

[9] J.N. Bailenson, N. Yee, S. Brave, D. Merget, and D. Koslow, "Virtual Interpersonal Touch: Expressing and Recognizing Emotions Through Haptic Devices," *Human Computer Interaction,* vol. 22, no. 3, pp. 325-353, 2007.

[10] J. Bailenson and N. Yee, "Virtual Interpersonal Touch: Haptic Interaction and Copresence in Collaborative Virtual Environments," *Multimedia Tools and Applications,* vol. 37, no. 1, pp. 5-14, 2008.

[11] J. Kim, H. Kim, B.K. Tay, M. Muniyandi, M.A. Srinivasan, J. Jordan, J. Mortensen, M. Oliveira, and M. Slater, "Transatlantic Touch: A Study of Haptic Collaboration over Long Distance," *Presence: Teleoperators and Virtual Environments,* vol. 13, no. 3, pp. 328-337, 2004.

[12] M. McLaughlin, G. Sukhatme, P. Wei, Z. Weirong, and J. Parks, "Performance and Co-Presence in Heterogeneous Haptic Collaboration," *Proc. 11th Symp. Haptic Interfaces for Virtual Environment and Teleoperator Systems (HAPTIC '03),* 2003.

[13] J.P. Hespanha, M. McLaughlin, G.S. Sukhatme, M. Akbarian, R. Garg, and W. Zhu, "Haptic Collaboration over the Internet," *Proc. Fifth PHANTOM Users Group Workshop,* 2000.

[14] S. Gentry, E. Feron, and R. Murray-Smith, "Human-Human Haptic Collaboration in Cyclical Fitts' Tasks," *Proc. IEEE/RSJ Int'l Conf. Intelligent Robots and Systems (IROS '05),* 2005.

[15] R. Groten, D. Feth, H. Goshy, A. Peer, D.A. Kenny, and M. Buss, "Experimental Analysis of Dominance in Haptic Collaboration," *Proc. IEEE 18th Int'l Symp. Robot and Human Interactive Comm. (RO-MAN '09),* 2009.

[16] N. Durlach and M. Slater, "Presence in Shared Virtual Environments and Virtual Togetherness," *Presence: Teleoperators and Virtual Environments,* vol. 9, no. 2, pp. 214-217, 2000.

[17] R. Ikeura, H. Inooka, and K. Mizutani, "Subjective Evaluation for Manoeuvrability of a Robot Cooperating with Human," *Proc. IEEE Eighth Int'l Workshop Robot and Human Interaction,* 1999.

[18] M.M. Rahman, R. Ikeura, and K. Mizutani, "Investigation of the Impedance Characteristic of Human Arm for Development of Robots to Cooperate with Humans," *JSME Int'l J. Series C Mechanical Systems, Machine Elements, and Manufacturing,* vol. 45, no. 2, pp. 510-518, 2002.

[19] Z. Wang, J. Lu, A. Peer, and M. Buss, "Influence of Vision and Haptics on Plausibility of Social Interaction in Virtual Reality Scenarios," *Haptics: Generating and Perceiving Tangible Sensations,* pp. 172-177, Springer, 2010.

[20] D. Feth, R. Groten, A. Peer, and M. Buss, "Haptic Human-Robot Collaboration: Comparison of Robot Partner Implementations in Terms of Human-Likeness and Task Performance," *Presence: Teleoperators and Virtual Environments,* vol. 20, no. 2, pp. 173-189, 2011.

[21] M. Jindai, T. Watanabe, S. Shibata, and T. Yamamoto, "Development of Handshake Robot System for Embodied Interaction with Humans," *Proc. IEEE 15th Int'l Symp. Robot and Human Interactive Comm.,* 2006.

[22] T. Kasuga and M. Hashimoto, "Human-Robot Handshaking Using Neural Oscillators," *Proc. Int'l Conf. Robotics and Automation,* 2005.

[23] K. Ouchi and S. Hashimoto, "Handshake Telephone System to Communicate with Voice and Force," *Proc. IEEE Int'l Workshop Robot and Human Comm.,* pp. 466-471, 1997.

[24] J.N. Bailenson and N. Yee, "Virtual Interpersonal Touch and Digital Chameleons," *J. Nonverbal Behavior,* vol. 31, no. 4, pp. 225-242, 2007.

[25] T. Miyashita and H. Ishiguro, "Human-Like Natural Behavior Generation Based on Involuntary Motions for Humanoid Robots," *Robotics and Autonomous Systems,* vol. 48, no. 4, pp. 203-212, 2004.

[26] Y. Kunii and H. Hashimoto, "Tele-Handshake Using Handshake Device," *Proc. IEEE 21st Ann. Conf. Industrial Electronics (IECON '95),* 1995.

[27] T. Sato, M. Hashimoto, and M. Tsukahara, "Synchronization Based Control Using Online Design of Dynamics and Its Application to Human-Robot Interaction," *Proc. IEEE Int'l Conf. Robotics and Biomimetics (ROBIO '07),* 2007.

[28] Z. Wang, A. Peer, and M. Buss, "An HMM Approach to Realistic Haptic Human-Robot Interaction," *Proc. Third Joint EuroHaptics Conf.* 2009.

[29] G. Loeb, I. Brown, and E. Cheng, "A Hierarchical Foundation for Models of Sensorimotor Control," *Experimental Brain Research,* vol. 126, no. 1, pp. 1-18, 1999.

[30] K.P. Kording and D.M. Wolpert, "Bayesian Decision Theory in Sensorimotor Control," *Trends in Cognitive Sciences,* vol. 10, no. 7, pp. 319-326, 2006.

[31] A.G. Feldman and M.F. Levin, "The Equilibrium-Point Hypothesis-Past, Present, and Future," *Progress in Motor Control,* vol. 629, pp. 699-726, 2009.

[32] R. Shadmehr and S.P. Wise, *The Computational Neurobiology of Reaching and Pointing: A Foundation for Motor Learning.* MIT Press, 2005.

[33] T. Flash and I. Gurevich, "Models of Motor Adaptation and Impedance Control in Human arm Movements," *Self-Organization, Comutational Maps, and Motor Control,* pp. 423-481, Elsevier Science, 1997.

[34] R. Shadmehr and F.A. Mussa-Ivaldi, "Adaptive Representation of Dynamics during Learning of a Motor Task," *J. Neuroscience,* vol. 14, no. 5, pp. 3208-3224, 1994.

[35] J.R. Flanagan and A.M. Wing, "The Role of Internal Models in Motion Planning and Control: Evidence from Grip Force Adjustments during Movements of Hand-Held Loads," *J. Neuroscience,* vol. 17, no. 4, pp. 1519-1528, 1997.

[36] J.R. Lackner and P. DiZio, "Rapid Adaptation to Coriolis Force Perturbations of Arm Trajectories," *J. Neurophysiology,* vol. 72, pp. 299-313, 1994.

[37] D.M. Wolpert and Z. Ghahramani, "Computational Principles of Movement Neuroscience," *Nature Neuroscience,* vol. 3, pp. 1212-1217, 2000.

[38] K.A. Thoroughman and R. Shadmehr, "Learning of Action through Adaptive Combination of Motor Primitives," *Nature,* vol. 407, no. 6805, pp. 742-747, 2000.

[39] A. Karniel and F.A. Mussa-Ivaldi, "Sequence, Time, or State Representation: How Does the Motor Control System Adapt to Variable Environments?" *Biological Cybernetics,* vol. 89, no. 1, pp. 10-21, 2003.

[40] H. Gomi and M. Kawato, "Equilibrium-Point Control Hypothesis Examined by Measured arm Stiffness during Multijoint Movement," *Science,* vol. 272, no. 5258, pp. 117-120, 1996.

[41] T. Flash and N. Hogan, "The Coordination of Arm Movements: An Experimentally Confirmed Mathematical Model," *J. Neuroscience,* vol. 5, no. 7, pp. 1688-1703, 1985.

[42] P. Morasso, "Spatial Control of Arm Movements," *Experimental Brain Research,* vol. 42, no. 2, pp. 223-227, 1981.

[43] T.B. Sheridan, "Further Musings on the Psychophysics of Presence," *Proc. IEEE Int'l Conf. Systems, Man, and Cybernetics, "Humans, Information and Technology,"* 1994.

[44] T.B. Sheridan, "Further Musings on the Psychophysics of Presence," *Presence: Teleoperators and Virtual Environments,* vol. 5, no. 2, pp. 241-246, 1996.

[45] G. Avraham, S. Levy-Tzedek, B.-C. Peles, S. Bar-Haim, and A. Karniel, "Reduced Frequency Variability in Handshake Movements of Individuals with Cerebral Palsy," *Proc. Sixth Computational Motor Control Workshop,* 2010.

[46] J.-F. Pilon and A. Feldman, "Threshold Control of Motor Actions Prevents Destabilizing Effects of Proprioceptive Delays," *Experimental Brain Research,* vol. 174, no. 2, pp. 229-239, 2006.

[47] R. Axelrod and W.D. Hamilton, "The Evolution of Cooperation," *Science,* vol. 211, no. 4489, pp. 1390-1396, 1981.

[48] A. Feldman, "Functional Tuning of the Nervous System with Control of Movement or Maintenance of a Steady Posture-II. Controllable Parameters of the Muscle," *Biophysics,* vol. 11, no. 3, pp. 565-578, 1966.
[49] J.F. Pilon and A.G. Feldman, "Threshold Control of Motor Actions Prevents Destabilizing Effects of Proprioceptive Delays," *Experimental Brain Research,* vol. 174, no. 2, pp. 229-239, 2006.
[50] A.G. Feldman and M.F. Levin, "The Origin and Use of Positional Frames of Reference in Motor Control," *Behavioral and Brain Sciences,* vol. 18, no. 4, pp. 723-744, 1995.
[51] P.L. Gribble, D.J. Ostry, V. Sanguineti, and R. Laboissi re, "Are Complex Control Signals Required for Human arm Movement?" *J. Neurophysiology,* vol. 79, no. 3, pp. 1409-1424, 1998.
[52] A.V. Hill, "The Heat of Shortening and the Dynamic Constants of Muscle," *Proc. Royal Soc. of London. Series B, Biological Sciences,* vol. 126, no. 843, pp. 136-195, 1938.
[53] G.A. Dudley, R.T. Harris, M.R. Duvoisin, B.M. Hather, and P. Buchanan, "Effect of Voluntary versus Artificial Activation on the Relationship of Muscle Torque to Speed," *J. Applied Physiology,* vol. 69, no. 6, pp. 2215-2221, 1990.
[54] Y. Yamato, M. Jindai, and T. Watanabe, "Development of a Shake-Motion Leading Model for Human-Robot Handshaking," *SICE Ann. Conf.,* 2008.
[55] C.M. Bishop, *Pattern Recognition and Machine Learning.* Springer, 2006.
[56] G.A. Gescheider, *Method, Theory, and Application.* Lawrence Erlbaum Associates, 1985.
[57] F. Wichmann and N. Hill, "The Psychometric Function: I. Fitting, Sampling, and Goodness of Fit," *Perception and Psychophysics,* vol. 63, no. 8, pp. 1293-1313, 2001.
[58] R. Davoodi and G.E. Loeb, "Physics-Based Simulation for Restoration and Rehabilitation of Movement Disorders," *IEEE Trans. Biomedical Eng.,* In press.
[59] K.J. Kuchenbecker, J.G. Park, and G. Niemeyer, "Characterizing the Human Wrist for Improved Haptic Interaction," *Proc. Int'l Mechanical Eng. Congress and Exposition (IMECE '03),* 2003.
[60] V.M. Zatsiorsky, *Kinetics of Human Motion.* Human Kinetics, 2002.
[61] C.L. Baker, R. Saxe, and J.B. Tenenbaum, "Action Understanding as Inverse Planning," *Cognition,* vol. 113, no. 3, pp. 329-349, 2009.
[62] F. Everett, N. Proctor, and B. Cartmell, "Providing Psychological Services to American Indian Children and Families," *Professional Psychology: Research and Practice,* vol. 14, no. 5, pp. 588-603, 1983.
[63] H.S. Woo and C. Prud'homme, "Cultural Characteristics Prevalent in the Chinese Negotiation Process," *European Business Rev.,* vol. 99, no. 5, pp. 313-322, 1999.
[64] C.M. Laine, K.M. Spitler, C.P. Mosher, and K.M. Gothard, "Behavioral Triggers of Skin Conductance Responses and Their Neural Correlates in the Primate Amygdala," *J. Neurophysiology,* vol. 101, no. 4, pp. 1749-1754, 2009.
[65] J. Anttonen and V. Surakka, "Emotions and Heart Rate While Sitting on a Chair," *Proc. SIGCHI Conf. Human Factors in Computing Systems,* pp. 491-499, 2005.
[66] J. Freeman, S.E. Avons, R. Meddis, D.E. Pearson, and W. IJsselsteijn, "Using Behavioral Realism to Estimate Presence: A Study of the Utility of Postural Responses to Motion Stimuli," *Presence: Teleoperators and Virtual Environments,* vol. 9, no. 2, pp. 149-164, 2000.
[67] D.W. Schloerb, "A Quantitative Measure of Telepresence," *Presence: Teleoperators and Virtual Environments,* vol. 4, no. 1, pp. 64-80, 1995.
[68] K.B. Reed and M.A. Peshkin, "Physical Collaboration of Human-Human and Human-Robot Teams," *IEEE Trans. Haptics,* vol. 1, no. 2, pp. 108-120, July-Dec. 2008.
[69] T. Ganel and M.A. Goodale, "Visual Control of Action but Not Perception Requires Analytical Processing of Object Shape," *Nature,* vol. 426, no. 6967, pp. 664-667, 2003.
[70] M.A. Goodale and A.D. Milner, "Separate Visoual Pathways for Perception and Action," *Trends in Neurosciences,* vol. 15, no. 1, pp. 20-25, 1992.
[71] S. Aglioti, J.F.X. DeSouza, and M.A. Goodale, "Size-Contrast Illusions Deceive the Eye but Not the Hand," *Current Biology,* vol. 5, no. 6, pp. 679-685, 1995.
[72] A. Pressman, I. Nisky, A. Karniel, and F.A. Mussa-Ivaldi, "Probing Virtual Boundaries and the Perception of Delayed Stiffness," *Advanced Robotics,* vol. 22, pp. 119-140, 2008.
[73] I. Nisky, A. Pressman, C.M. Pugh, F.A. Mussa-Ivaldi, and A. Karniel, "Perception and Action in Teleoperated Needle Insertion," *IEEE Trans. Haptics,* vol. 4, no. 3, pp. 155-166, May-June 2011.
[74] P. Tuffield and H. Elias, "The Shadow Robot Mimics Human Actions," *Industrial Robot: An Int'l J.,* vol. 30, no. 1, pp. 56-60, 2003.
[75] H. Liu, P. Meusel, N. Seitz, B. Willberg, G. Hirzinger, M. Jin, Y. Liu, R. Wei, and Z. Xie, "The Modular Multisensory DLR-HIT-Hand," *Mechanism and Machine Theory,* vol. 42, no. 5, pp. 612-625, 2007.
[76] N. Wettels, V.J. Santos, R.S. Johansson, and G.E. Loeb, "Biomimetic Tactile Sensor Array," *Advanced Robotics,* vol. 22, no. 8, pp. 829-849, 2008.
[77] J.C. van der Heide, J.M. Fock, B. Otten, E. Stremmelaar, and M. Hadders-Algra, "Kinematic Characteristics of Reaching Movements in Preterm Children with Cerebral Palsy," *Pediatric Research,* vol. 57, no. 6, p. 883, 2005.
[78] L. Roennqvist and B. Roesblad, "Kinematic Analysis of Unimanual Reaching and Grasping Movements in Children with Hemiplegic Cerebral Palsy," *Clinical Biomechanics,* vol. 22, no. 2, pp. 165-175, 2007.
[79] B. van Den, "Coordination Disorders in Patients With Parkinson's Disease: A Study of Paced Rhythmic Forearm Movements," *Experimental Brain Research,* vol. 134, no. 2, pp. 174-186, 2000.

Guy Avraham received the BSc (magna cum laude) degree from the Department of Life Science, The Hebrew University of Jerusalem, Israel, in 2008, and the MSc degree from the Department of Biomedical Engineering, Ben-Gurion University of the Negev, Israel, in 2011. He received the Science Faculty Dean's Award for Excellence from the Hebrew University of Jerusalem in 2008.

Ilana Nisky received the BSc (summa cum laude), MSc (summa cum laude), and PhD degrees from the Department of Biomedical Engineering, Ben-Gurion University of the Negev, Israel, in 2006, 2009, and 2011, respectively. Currently, she is a postdoctoral research fellow in the Department of Mechanical Engineering, Stanford University. She received the Wolf Foundation scholarship for undergraduate and graduate students, Zlotowski, and Ben-Amitai prizes for excellent graduate research, Kreitman Foundation Fellowship, Clore scholarship, and the Wezmann Institute of Science national postdoctoral award for advancing women in science. Her research interests include motor control, haptics, robotics, human, and machine learning, teleoperation, and human-machine interfaces. She is a member of the Society for the Neural Control of Movement, the Society for Neuroscience, Technical Committee on Haptics, and EuroHaptics Society.

Hugo L. Fernandes received the BSc degree in mathematics and the MSc degree in applied mathematics from the Faculty of Science of the University of Porto, Portugal, in 2001 and 2004, respectively. Currently, he is working toward the PhD degree in computational biology, Instituto Gulbenkian de Cincia, Oeiras, Portugal. Since 2009, he has been doing his research at the Bayesian Behavior Lab, Northwestern University, Chicago. His main research interests include how information, in particular uncertainty, is represented and processed in the brain.

Daniel E. Acuna received the bachelor and master's degrees from the University of Santiago, Chile and the PhD degree from the University of Minnesota-Twin Cities, Minnesota. Currently, he is a research associate in the Sensory Motor Performance Program (SMPP) at the Rehabilitation Institute of Chicago and Northwestern University. During his PhD, he received a NIH Neuro-physical-computational Sciences (NPCS) Graduate Training Fellowship (2008-2010) and an International Graduate Student Fellowship from the Chilean Council of Scientific and Technological Research and the World Bank (2006-2010). His research interests include sequential optimal learning and control, brain machine interfaces, and hierarchical motor control.

Konrad P. Kording received the PhD degree in physics from the Federal Institute of Technology (ETH), Zurich, Switzerland, where he worked on cat electrophysiology and neural modeling. He received postdoctoral training in London where he worked on motor control and Bayesian statistics. Another postdoc, partially funded by a German Heisenberg stipend, followed at MIT where he worked on cognitive science and natural language processing and deepened his knowledge of Bayesian methods. Since 2006, he has been working for the Rehabilitation Institute of Chicago and Northwestern University where he received tenure and promotion to associate professor in 2011. His group is broadly interested in uncertainty, using Bayesian approaches to model human behavior and for neural data analysis.

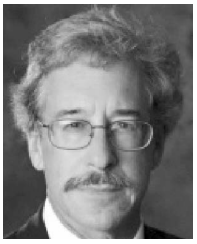

Gerald E. Loeb (M'98) received the BA and MD degrees from Johns Hopkins University, in 1969 and 1972, respectively, and did one year of surgical residency at the University of Arizona before joining the Laboratory of Neural Control at the National Institutes of Health (1973-1988). He was a professor of physiology and biomedical engineering at Queen's University in Kingston, Canada (1988-1999) and is now a professor of biomedical engineering and the director of the medical device development facility at the University of Southern California (http://mddf.usc.edu). He was one of the original developers of the cochlear implant to restore hearing to the deaf and was chief scientist for Advanced Bionics Corp. (1994-1999), manufacturers of the Clarion cochlear implant. He is a fellow of the American Institute of Medical and Biological Engineers, holder of 54 issued US patents and author of more than 200 scientific papers available at http://bme.usc.edu/gloeb. Most of his current research is directed toward sensorimotor control of paralyzed and prosthetic limbs. His research team developed BION injectable neuromuscular stimulators and has been conducting several pilot clinical trials. They are developing and commercializing a biomimetic tactile sensor for robotic and prosthetic hands through a start-up company for which he is chief executive officer (www.SynTouchLLC.com). His laboratory at USC is developing computer models of musculoskeletal mechanics and the interneuronal circuitry of the spinal cord, which facilitates control and learning of voluntary motor behaviors by the brain. These projects build on his long-standing basic research into the properties and natural activities of muscles, motoneurons, proprioceptors, and spinal reflexes. He is a senior member of the IEEE.

Amir Karniel received the BSc (cum laude), MSc, and PhD degrees in 1993, 1996, and 2000, respectively, all in electrical engineering from the Technion-Israel Institute of Technology, Haifa, Israel. He had been a postdoctoral fellow at the Department of Physiology, Northwestern University Medical School and the Robotics Lab of the Rehabilitation Institute of Chicago. Currently, he is an associate professor in the Department of Biomedical Engineering at Ben-Gurion University of the Negev where he serves as the head of the Computational Motor Control Laboratory and the organizer of the annual International Computational Motor Control Workshop. He received the E. I. Jury Award for excellent students in the area of systems theory, and the Wolf Scholarship Award for excellent research students. In the last few years, his studies are funded by awards from the Israel Science Foundation, The Binational US Israel Science Foundation, and the US-AID Middle East Research Collaboration. He is on the editorial board of the *IEEE Transactions on System Man and Cybernetics Part A*, and the *Frontiers in Neuroscience*. His research interests include human-machine interfaces, haptics, brain theory, motor control and motor learning. He is a senior member of the IEEE.